Journal of the Korean Ceramic Society
Vol. 43, No. 11, pp. 673~679, 2006.

Review

Theoretical Aspects of PTC Thermistors

Sang-Hee Cho†

Department of Inorganic Materials Engineering, Kyungpook National University, Daegu 702-701, Korea
(Received October 19, 2006; Accepted October 31, 2006)

ABSTRACT

The discovery of ferroelectric barium titanate ($BaTiO_3$) in 1942 began the present era of dielectrics-based electronic ceramics. Ferroelectric barium titanate has a high dielectric constant and after the recognition of $BaTiO_3$ as a new ferroelectric compound, various attractive electrical properties have been extensively studied and reported. Since then, pioneering work on valence-compensated semiconduction led to the discovery of the positive temperature coefficient (PTC) of the resistance effect found in doped $BaTiO_3$. Significant progress has since followed with respect to understanding the PTC phenomena, advancing materials capabilities, and developing devices for sensor and switching applications. In this paper, the theoretical aspects of the various PTC models are discussed and the future trends of practical applications for PTC devices are briefly mentioned.

Key words : PTC, Thermistor, $BaTiO_3$, Semiconducting

1. Theoretical Background of the PTC

1.1. Heywang Model

Semiconducting barium titanate ($BaTiO_3$) positive temperature coefficient (PTC) ceramics are widely used as temperature sensors, self-regulating heaters, over-current and over-temperature protectors, and degaussers due to their unique R-T, I-V, and I-t characteristics. The PTC effect is known to have originated due to the electrical back-to-back double Schottky barrier at the grain boundary, which was suggested by Heywang.[1,2]

The Heywang model is the most accepted model when explaining $BaTiO_3$-based PTC devices.[3,4] Heywang assumed a two dimensional layer of acceptor states along the grain boundaries. These acceptors attract electrons from the bulk, resulting in an electron depletion layer with a width of d,

$$d=\frac{N_S}{2N_d}, \tag{1}$$

where N_S is the density of the acceptor states at the grain boundaries and N_d is the charge carrier concentration, as shown in Fig. 1. The depletion layer results in a grain boundary potential barrier φ_o are:

$$\varphi_o=\frac{eN_S^2(T)}{8\varepsilon_o\varepsilon_{gb}(T)N_d}, \tag{2}$$

where e is the electron charge, ε_o is the permittivity of free space, and ε_{gb} is the relative permittivity of the grain boundary region. In equation (2), N_S and ε_{gb} are a function of the temperature.

The temperature dependence of the active acceptor state density, N_S, is described by:

$$N_S(T)=\frac{N_{So}}{1+\exp\frac{(E_F+e\varphi_o-E_S)}{kT}}, \tag{3}$$

where N_{So} is the number of acceptor states, E_S is the energy gap between the energy levels of the acceptor states, k is the Boltzmann constant and conduction band, and E_F is the Fermi energy which equals

$$E_F=kT\ln\left(\frac{N_C}{N_d}\right), \tag{4}$$

where N_C is the effective density of the states in the conduction band. ε_{gb} follows the Curie-Weiss law:

$$\varepsilon_{gb}=\frac{C}{T-\theta} \tag{5}$$

where C is the Curie-Weiss constant and θ is the Curie-Weiss temperature.

The resistivity of the samples, ρ, is related to the potential

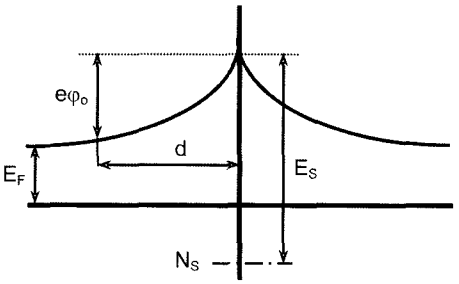

Fig. 1. Double Schottky barrier at the grain boundary caused by a two dimensional acceptor layer along the grain boundary. After Heywang.[1,2]

†Corresponding author : Sang-Hee Cho
E-mail : shcho@knu.ac.kr
Tel : +82-53-950-6593 Fax : +82-53-955-8179

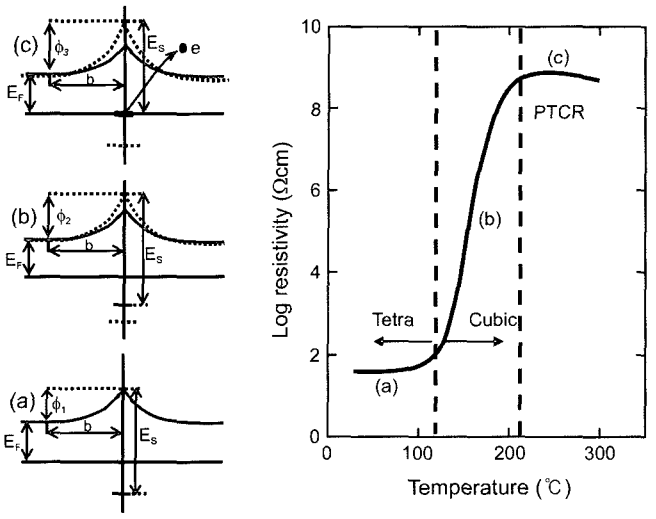

Fig. 2. Simplified energy band diagrams at a grain boundary with electrons trapped by the acceptor states of the energy level E_S: (a) below T_C, (b) $T_C<T<T_{max}$, and (c) $T>T_{max}$.

barrier, as in the following equation where R is a constant:

$$\rho = R \cdot \exp\left(\frac{e\varphi_o}{kT}\right). \quad (6)$$

At $T=\theta$, the acceptor levels are well below the Fermi level and filled so that $N_S=N_{So}$. Due to the decrease of permittivity in the grain boundary region resulting from the phase transition of $BaTiO_3$ ceramics from ferroelectric to paraelectric above the Curie temperature, the potential φ_o increases proportionally with the temperature as expressed in equations (2) and (5) (see Fig. 2). The acceptor states (E_S) are raised simultaneously with the potential barrier at the grain boundaries and as the temperature increases above the Curie point, which corresponds to Fig. 2(b), the resistivity increases due to the increased potential barrier. When the E_S reach the Fermi level, where the maximum resistivity is obtained at T_{max}, the trapped electrons begin to jump to the conduction band, resulting in an increase in φ_o and ρ, and reducing the resistivity (see Fig. 2(c)).

An increase in E_S causes a rise in ρ_{max} because the energy gap between the acceptor states and the Fermi level is larger. The temperature at which the electrons have sufficient energy to jump to the conduction band is higher, and therefore, ρ_{max} and T_{max} are increased by an increase in E_S. ρ_{max} is also increased by a rise in N_S, as can be seen in Fig. 3.[5] At the Curie temperature, T_C, the potential barrier is higher when N_S is higher. When E_S is fixed, the energy gap between the Fermi level and the acceptor states' energies decreases with an increasing N_S. This shows that with a rising temperature, the acceptors reach the Fermi level at a lower temperature, which leads to a decrease in T_{max}.

On the other hand, Nemoto *et al.*[6] and Sumino *et al.*[7] measured the resistance of the single grain boundaries using a specially designed instrument with two thin Al

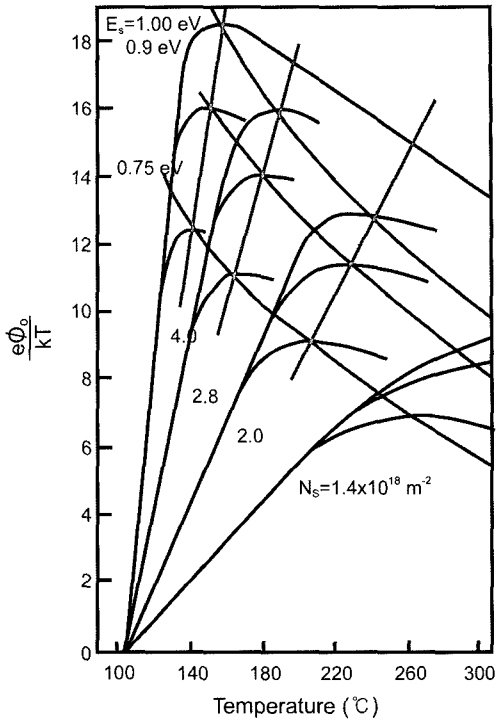

Fig. 3. Calculated $e\varphi_o/kT$ curves. The ρ_{max} increases and T_{max} decreases from an increase in acceptor density, N_S. ρ_{max} and T_{max} both increase from an increase in E_S. After Jonker.[5]

wires (25~30 μm in diameter). The two wires were welded either to the same grain or to two adjacent grains. In the latter case, there was only one grain boundary between the two wires. It was found that the grains showed a Negative Temperature Coefficient (NTC) while the grain boundaries showed a PTC. However, the PTC jump was different for every grain boundary. This is attributed to a difference in the N_S and/or N_d.[6] These results prove that the PTC is a grain boundary phenomenon that can be qualitatively explained using the Heywang model assuming a two dimensional plane of acceptor states at the grain boundaries. Although the Heywang model gives a good description and explanation of the PTC behavior, it leaves some questions unanswered. Some of these questions are:

1. What is the precise nature of the acceptor states?
2. Why does the PTC effect only occur in semiconductive materials generated by doping? Why doesn't it appear in semiconductive materials generated by reduction?
3. Why is the PTC significantly affected by the cooling process after sintering and by heat treatments?
4. What is the explanation for the origin of the peculiar behavior where the conductivity of $BaTiO_3$ rises only if small dopant concentrations are added and decreases if large concentrations are added?

1.2. Daniel Model[8]

In order to achieve better control over the PTC characteristics, Daniels *et al.*[8] developed a model in order to find

answers for the unanswered questions left by the Heywang model.[8] The Daniel model will be explained in a similar way to the way Daniels *et al.* explained it in the reference.[8] A more detailed description can be found in other sources.[9-13] After studying the thermodynamic equilibrium during sintering and the kinetic processes during cooling, Daniels and Wernicke concluded that the PTC effect is caused by the defect distribution in the samples.

To calculate the equilibrium defect concentration, Daniels et al. assumed the following defects in $BaTiO_3$: neutral, single, and double ionized oxygen vacancies (V_O, $V_O^{\cdot}$, and $V_O^{\cdot\cdot}$), and neutral, single, and double ionized barium vacancies (V_{Ba}, V'_{Ba}, and V''_{Ba}). It was also assumed that the amount of Ti vacancies was negligible. When a donor dopant is incorporated into the lattice, e.g. La^{3+} on Ba^{2+} sites or Nb^{5+} on Ti^{4+} sites, the extra charge must be compensated. This can be achieved through vacancies or electrons. With the above defects, the electroneutrality can be written as:

$$n+[V'_{Ba}]+2[V''_{Ba}]=p+[V_O^{\cdot}]+[V_O^{\cdot\cdot}]+[La^{+}] \qquad (7)$$

where n is the electron concentration and p is the hole concentration. The reaction equations and equilibrium conditions for La-doped $BaTiO_3$ follow.[5]

$$O(lattice) \Leftrightarrow V_O + O_2 \qquad [V_O]P_{O_2} = K_1$$

$$V_O \Leftrightarrow V_O^{\cdot} + e \qquad [V_O^{\cdot}]n/[V_O] = K_2$$

$$V_O^{\cdot} \Leftrightarrow V_O^{\cdot\cdot} + e \qquad [V_O^{\cdot\cdot}]n/[V_O^{\cdot}] = K_3$$

$$V_{Ba} \Leftrightarrow V'_{Ba} + h \qquad [V'_{Ba}]p/[V'_{Ba}] = K_4$$

$$V'_{Ba} \Leftrightarrow V''_{Ba} + h \qquad [V''_{Ba}]p/[V'_{Ba}] = K_5$$

$$La \Leftrightarrow La^{+} + e \qquad [La^{+}]n/[La] = K_D$$

$$e + h = 0 \qquad np = K_i$$

$$BaTi_3O_7 + 2Ba(lattice) + 2O(lattice) \Leftrightarrow 3BaTiO_3 + 2V_{Ba} + 2V_O$$

It has been suggested that titanates with a higher TiO_2 concentration are present at the grain boundaries; therefore, the final reaction should be considered as an example. Ba_2TiO_4 is another possible grain boundary phase; however, a reaction similar that above can be written for this compound.[12]

With these equations, the equilibrium concentrations are calculated for different temperatures and P_{O_2}. The result of these calculations is given in Fig. 4, which clearly shows three different areas with different charge compensation mechanisms:

$$2*[V''_{Ba}] \approx [La^{+}] \quad \text{I},$$
$$n \approx [La^{+}] \quad \text{II, and}$$
$$n \approx [V_O^{\cdot}] \quad \text{III}.$$

In region III, the reduction is so severe that the number of

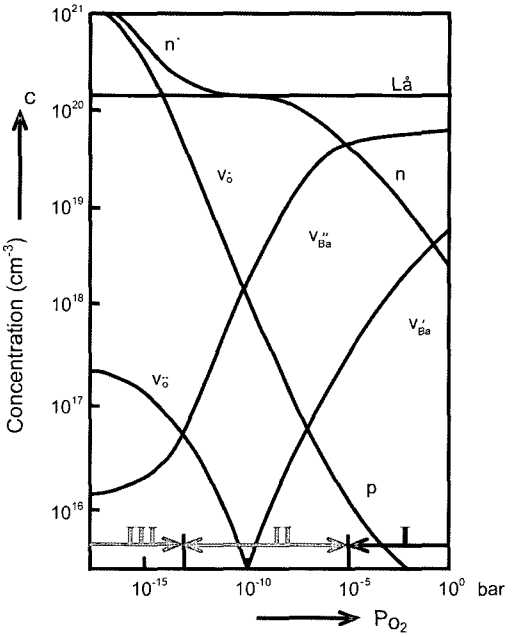

Fig. 4. The concentrations of all defects calculated as a function of the oxygen partial pressure at 1200°C, on samples of $BaTiO_3$ doped with 1% La. After Daniels *et al.*[8]

electrons equals the number of oxygen vacancies. This is similar to the reduction in non-doped $BaTiO_3$. In regions II and III, the donors are compensated by electrons and barium vacancies, respectively. When one changes the P_{O_2} or temperature, $BaTiO_3$ will restore its equilibrium by the creation, annihilation, and/or diffusion of the defects. In non-doped $BaTiO_3$, oxygen diffusion is the rate controlling step. The oxygen vacancies are formed or annihilated at the surface of the sample and diffused inward.

Diffusion experiments have shown that the equilibration process in the case of donor-doped $BaTiO_3$ is different. After changes in the P_{O_2} or temperature, the oxygen vacancies attain a new equilibrium concentration, and then V_{Ba} are formed at the grain boundary and are diffused from the grain boundaries into the grain in order to attain an equilibrium concentration. Therefore, the diffusion of the V_{Ba} is the rate controlling step during equilibration

During cooling from the sintering temperature, the donor-doped $BaTiO_3$ tends to stay in equilibrium with the atmosphere. As the equilibrium barium vacancy (V_{Ba}) concentration increases with the decreasing temperature, the overall V_{Ba} concentration increases. The V_{Ba} are produced at the grain boundaries and are diffused from the grain boundaries into the grain. Due to the slow V_{Ba} diffusion, the inside of the grains cannot equilibrate with the surrounding atmosphere below a certain temperature. This indicates that the V_{Ba} rich diffusion front comes to a standstill. However, the grain boundary region retains its equilibrium V_{Ba} concentration until quite low temperatures. Therefore, the result after cooling is a sample with conducting grains surrounded by an insulating barium vacancy rich grain boundary layer,

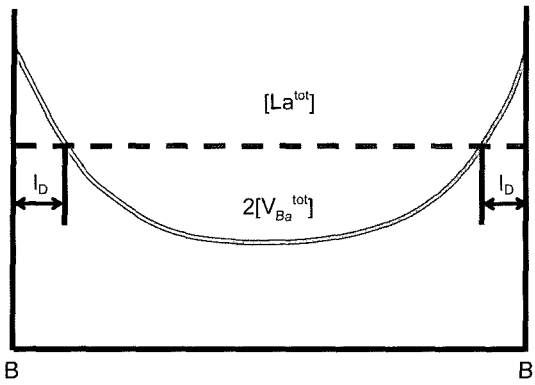

Fig. 5. Schematic profile of the V_{Ba} rich insulating grain boundary layer. The V_{Ba} diffuses inward from the grain boundary and compensates the extra donor charge where the layer becomes insulating. I_D is the width of the insulating layer and B is the grain boundary. After Daniels *et al.*[8]

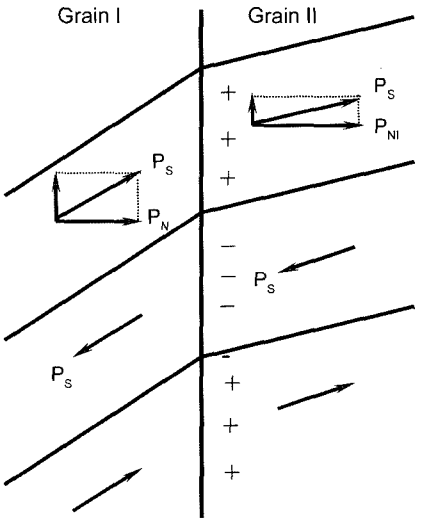

Fig. 6. A schematic illustrating the polarization of the ferroelectric domains at the grain boundary. After Jonker.[14]

as shown in Fig. 5.

With this model, Daniels *et al.* could explain the questions left unanswered by the Heywang model. Daniels and Wernicke claimed that the V_{Ba} act as accepters and trap electrons from the bulk, creating a potential barrier. As the semiconductive $BaTiO_3$ only generated by reduction contains oxygen vacancies, there is no PTC in this type of material. The PTC effect depends largely on the thickness I_D of the V_{Ba} rich grain boundary layer. The slower the cooling, the wider the layer will form. This shows that the V_{Ba} concentration will be greater. If the cooling rate is sufficiently slow, the doped $BaTiO_3$ will become an insulator, and the PTC effect will vanish.

The conductivity anomaly is explained by the Daniels model as follows. It is known that high dopant concentrations lead to small grain sizes, generally a few micron in size. At practical cooling rates, the insulating grain boundary layer is approximately 1 to 3 μm thick. Therefore, the small grained materials become an insulator at normal cooling rates.

A problem rises here because the low resistance of a PTC device at room temperature (below the Curie point) cannot be explained by either the Heywang model or the Daniel model. Therefore, the Jonker model[14] is usually used in combination with these models.

1.3. Jonker Model

Below the Curie point, $BaTiO_3$ becomes ferroelectric with its polarization axis aligned with the tetragonal crystal axis. The polarization changes direction from domain to domain, as seen schematically in Fig. 6.[14]

As adjacent grains have different crystal orientations, the polarization direction is also different from grain to grain. The difference in polarization direction causes a net polarization perpendicular to the grain boundaries and creates surface charges at the grain boundaries. For negative surface charges, which occupy approximately 50% of the grain boundary area, the depletion layer is partially or completely filled. Consequently, the charge barrier height diminishes or disappears. In 50% of the cases, the surface charge is positive, which creates an even higher potential. However, this does not matter as the conducting electrons always emulate the lowest barrier.

1.4. Effect of 3d Elements

Small additions of 3d elements, like Fe, Cr, and Mn, improve the PTCR behavior considerably.[15-19] It may be thought that the dopants influence the oxygen adsorption at the grain boundaries; however, it is unlikely that the additions of 3d elements in the range of 0.01 to 0.5 at%, as commonly used in PTC materials, influence the adsorption of gases at the grain boundaries. Moreover, different acceptor energy levels have been found for non-acceptor doped $BaTiO_3$ samples and $BaTiO_3$ samples doped with different 3d elements.[15,18] This shows that the adsorbed gases cannot be the only acceptors in $BaTiO_3$ PTC materials doped with 3d elements.

Daniels and Wernicke explained the influence of 3d elements as follows. Small additions of 3d elements with energy levels similar to or higher than the energy level of the double ionized barium vacancy make the insulating layer thicker, resulting in a change in the PTC behavior. Eventual segregation can alter the PTC property slightly, but it does not change the overall principal.[9] Also, this model does not explain the difference in E_S for different 3d elements and non-acceptor doped PTC materials. Therefore, this model can also be discarded as an explanation for the PTC enhancement by 3d elements.

Ueoka[16] proposed a model for Mn additions and it can also be applied to other acceptors. Ueoka claimed that during sintering the Mn present as Mn^{2+} on the Ti sites is compensated by oxygen vacancies. During cooling, the grain boundaries oxidize and Mn^{2+} changes its oxidation state to Mn^{3+} or

Mn^{4+}, which have deeper acceptor levels. Later, Hagemann *et al.* confirmed this possibility. Hagemann *et al.* found through the magnetic susceptibility and weight measurement changes of acceptor doped $BaTiO_3$, that Mn, Cr, and Co reversibly change their oxidation state when annealed at different oxygen partial pressures, while other 3d elements did not. At low P_{O_2}, when the acceptors have low oxidation states, less than 4, and are compensated by double ionized vacancies, the oxidation state changes are inseparably connected with the concentration of double ionized oxygen vacancies.[20,21]

On the other hand, Lee *et al.*[22] explained the role of Mn in $BaTiO_3$ based PTC materials as one where Mn occupies the Ti site, as in other previous studies,[22-25] and appears and segregates near the grain boundaries. In Lee's paper, the valence state of Mn was analyzed by ESR, and it was confirmed that the valence of Mn changes near the Curie point of $BaTiO_3$ from +3 in a tetragonal phase to 2+ in a cubic phase. Therefore, the number of electron traps increases at the Curie point, leading to a significant improvement in the PTC effect. The valence change of Mn ions explained the disappearance of the Jahn-Teller effect as the phase changed from tetragonal to cubic.

However, the possibility of V_{Ba} as acceptors should not be discarded. Using cathode luminescence (CL), Koschek *et al.* visualized the grain boundary area of a PTC device.[27,28] The grain boundary area appeared dark and the grains were light in the CL images with a multi-alkali-photomultiplier (spectral range 300~800 nm). However, in the CL images taken using a Ge detector (spectral range 850~1800 nm), the grain boundary area appeared light and the grains were dark.[27] In the spectral cathode luminescence, the grain had only one intensity peak at 500 nm.[28] However, the grain boundary area had two peaks: one at 500 nm and one at 850 nm. These results were explained by an extra energy level in the energy gap, corresponding to the energy level of the double ionized barium vacancies. The fast cooling also resulted in smaller grain boundary zones that did not surround the entire grains. As the fast-cooled samples had a lower room temperature resistivity than the slow-cooled samples, Koschek *et al.* concluded that there is a correlation between the microscopic V_{Ba} rich grain boundary area and the macroscopic resistance properties.[27,28] With the current knowledge, it can be concluded that the acceptor, as well the adsorbed gases, can be 3d elements the same as V_{Ba}.

2. Processing Parameters in PTC Manufacturing

It is well known that the characteristics of PTC devices can change easily as a result of various processing parameters such as sintering conditions (temperature, oxygen partial pressure), donor concentrations, cooling rates, additives, porosities, mean grain sizes, heat treatments, and so on. However, it is noteworthy that these parameters are not directly correlated to the PTC characteristics. These indirect parameters affect the N_d (donor concentration), N_S (acceptor state density), and E_S (depth of acceptor level), which are regarded as the direct parameters in PTC properties. Fig. 7 shows an approximate inter-relationship between the indirect and direct parameters, which have a complex correlation with each other.

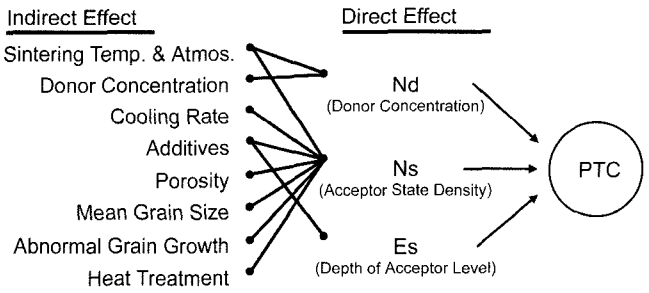

Fig. 7. The processing parameters affect the physical and chemical properties of the grain boundaries and finally influence the PTC properties. The most important factors that directly correlated with the PTC properties are N_d, N_S, and E_S.

3. New Demands in PTC Markets

Since the first observation of the PTC effect some decades ago, PTC devices have been used in various application areas. One of the largest applications has been in degaussers for color televisions, which erase the magnetic signals recorded on the television monitors by the Earth's magnetism and afterimages. Recent trends in the display market have shifted from CRT to flat panel displays. Worldwide demand for materials used in flat panel displays is expected to exhibit strong growth, more than offsetting the decline in demand for CRT materials. Therefore, the need for PTC degaussers will decrease. In order to create new PTC markets, more diverse uses and more sppealing characteristics of PTCs are necessary. Therefore, low resistance, durability at high voltage without electrical breakdown, and high accuracy are characteristics that must be satisfied to diversify the uses. A challenge to diversify the uses of PTCs will begin with the development of a low resistance PTC, below 1 Ohm at room temperature, using the MLCC technique. Since a low resistance consumes a low power, this PTC can be used in many battery powered portable devices. Polymeric PTC devices, which have been used to prevent overheating in various secondary batteries, could be replaced by a low resistance ceramic PTC. Fig. 8 shows the R-T characteristics of a newly developed multi-layered PTC that demonstrates a room temperature resistance near 0.5 Ohm. The inset of Fig. 8 shows the magnified view of the multi-layer structure in a multi-layered PTC.

Another potential new market is the automobile air conditioning and heating units, which have not yet been realized due to the unverified durability (more than 10 years in various harsh conditions) of PTC devices. As soon as the long term quality of the PTC devices is confirmed, a consumer

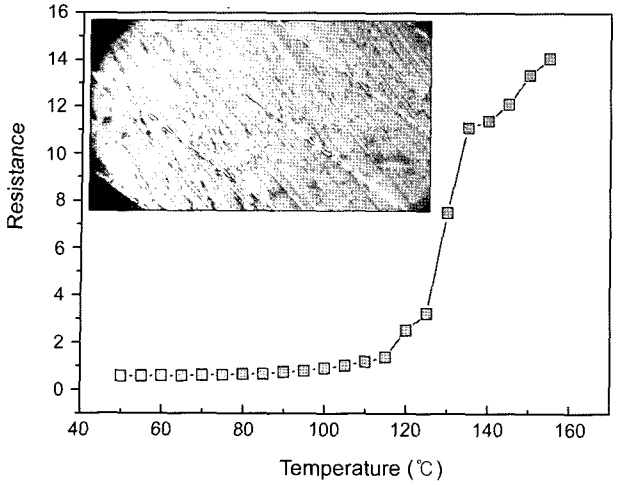

Fig. 8. The R-T characteristics of a multi-layered PTC device. The inset shows a magnified view of the multi-layer structure of the PTC (Courtesy of Ja Hwa Electronics Co., Ltd.).

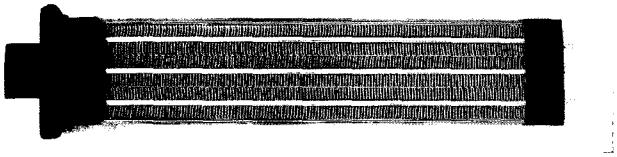

Fig. 9. A PTC heating device for use in automobiles to instantly heat air (Courtesy of Ja Hwa Electronics Co., Ltd.).

will not need to wait until the engine is warmed for warm air in a cold car because instantaneous heating will be available using the PTC devices. Fig. 9 shows a photograph of the PTC heater for automobiles.

4. Concluding Remarks

The fundamental theories of the PTC effect using the Heywang, Daniel, and Jonker models were examined. Unfortunately, there is no single theoretical model that can explain the entire PTC phenomenon completely. Therefore, the three models are always employed together to compensate for their theoretical incompleteness and weaknesses. Modification of the existing theories and creation of new practical applications for PTC devices are expected from the continuing research.

REFERENCES

1. W. Heywang, "Barium Titanate as a Semiconductor with Blocking Layer," *Sol. State Electron.*, **3** 51-8 (1961).
2. W. Heywang, "Resistivity Anomaly in Doped Barium Titanate," *J. Am. Ceram. Soc.*, **47** [10] 484-90 (1964).
3. B. Huybrechts, PhD. Thesis, Nagaoka University of Technology, Japan, 1994.
4. B. Huybrechts, K. Ishizaki, and M. Takata, "Review: The Positive Temperature Coefficient of Resistivity in Barium Titanate," *J. Mat. Sci.*, **30** 2463-74 (1995).
5. G. H. Jonker, "Halogen Treatment of Barium Titanate Semiconductors," *Mater. Res. Bull.*, **2** 401-07 (1967).
6. H. Nemoto and J. Oda, "Direct Examination of PTC Action of Single Grain Boundaries in Semiconducting $BaTiO_3$ Ceramics," *J. Am. Ceram. Soc.*, **63** [7-8] 393-401 (1980).
7. H. Sumino, O. Sakurai, K. Shinozaki, and N. Mizutani, "Direct Measurement of the PTC Effect of a Single Grain Boundary," *J. Ceram. Soc. of Jpn.*, **100** [1] 97-100 (1992).
8. J. Daniels, K. H. Hardtl, and R. Wernicke, "The PTC Effect of Barium Titanate," *Philips Tech. Rev.*, **38** [3] 73-82 (1978/79).
9. J. Daniels and R. Wernicke, "Part V. New Aspects of an Improved PTC Model," *Philips Res. Rep.*, **31** 544-59 (1976).
10. J. Daniels, "Part II. Defect Equilibria in Acceptor Doped Barium Titanate," *Philips Res. Rep.*, **31** 505 (1976).
11. J. Daniels and K. H. Hardtl, "Part I. Electrical Conductivity at High Temperatures of Donor Doped Barium Titanate Ceramics," *Philips Res. Rep.*, **31** 489 (1976).
12. R. Wernicke, "Part IV. The Kinetics of Equilibrium Restoration in Barium Titanate Ceramics," *Philips Res. Rep.*, **31** 526 (1976).
13. D. Hennings, "Part III. Thermogravimetric Investigations," *Philips Res. Rep.*, **31** 516 (1976).
14. G. H. Jonker, "Some Aspects of Semiconducting Barium Titanate," *Solid State Electron.*, **7** 895-903 (1964).
15. H. M. Al-Allak, A. W. Brinkman, G. J. Russel, and J. Woods, "The Effect of Mn on the Positive Temperature Coefficient of Resistance Characteristics of Donor Doped $BaTiO_3$ Ceramics," *J. Appl. Phys.*, **63** [9] 4530-35 (1988).
16. H. Ueoka, "The Doping Effects of Transition Elements on the PTC Anomaly of Semiconductive Ferroelectric Ceramics," *Ferroelectrics*, **7** 351-53 (1974).
17. H. Ueoka and M. Yodogawa, "Ceramic Manufacturing Technology for the High Performance PTC Thermistor," *IEEE Trans. Manuf. Tech.*, **3** [2] 77-82 (1974).
18. H. Ihrig, "PTC Effect in $BaTiO_3$ as a Function of Doping with 3d Elements," *J. Am. Ceram. Soc.*, **64** [10] 617-20 (1981).
19. T. Matuoka, Y. Matuo, H. Sasaki, and S. Hayakawa, "PTCR Behavior of $BaTiO_3$ with Nb_2O_5 and MnO_2 Additives," *J. Am. Ceram. Soc.*, **55** [2] 108 (1972).
20. H. J. Hagemann and H. Ihrig, "Valance Change and Phase Stability of 3d Doped $BaTiO_3$ Annealed in Oxygen and Hydrogen," *Phys. Rev. B*, **20** [9] 3871-78 (1979).
21. H. J. Hagemann and D. Hennings, "Reversible Weight Change of Acceptor Doped $BaTiO_3$," *J. Am. Ceram. Soc.*, **64** [10] 590-93 (1981).
22. J. H. Lee, S. H. Kim, and S. H. Cho, "Valency Change of Mn Ions in $BaTiO_3$-Based PTCR Materials," *J. Am. Ceram. Soc.*, **78** [10] 2845-48 (1995).
23. H. Ihrig, "The Phase Stability of $BaTiO_3$ as a Function of Doped 3d Elements: An Experimental Study," *J. Phy. C: Solid State Phys.*, **11** [4] 819-27 (1978).
24. Y. M. Chiang and T. Takagi, "Grain-Boundary Chemistry of Barium Titanate and Strontium Titanate: I, High Temperature Equilibrium Space Charge," *J. Am. Ceram. Soc.*, **73** [11] 3278-85 (1990).

25. M. Nakahara and T. Murakami, "Electron Status of Mn Ions in $Ba_{0.97}Sr_{0.03}TiO_3$ Single Crystals," *J. Appl. Phys.*, **45** [9] 3795-800 (1974).
26. I. Burn, "Mn-Doped Polycrystalline $BaTiO_3$," *J. Mater. Sci.*, **14** 2453-58 (1979).
27. G. Koschek and E. Kubalek, "Grain Boundary Characteristics and their Influence on the Electrical Resistance of Barium Titanate Ceramics," *J. Am. Ceram. Soc.*, **68** [11] 582-85 (1985).
28. G. Koschek, "A Contribution to the Microanalysis of Acceptor States at the Grain Boundaries in Barium Titanate Ceramics," *Deutschen Keramischen Gesellschaft,* **66** [3/4] 128 (1989).